

Feature Review

Applications of Spherical Nucleic Acid Nanoparticles as Delivery Systems

Ahad Mokhtarzadeh,^{1,2} Hassan Vahidnezhad,³ Leila Youssefian,^{3,4} Jafar Mosafer,⁵ Behzad Baradaran,^{1,*} and Jouni Uitto^{3,*}

Spherical nucleic acids (SNAs) are nanostructures consisting of highly oriented, dense layers of oligonucleotides arranged in a spherical 3D geometry. Owing to their unique properties and function, SNAs occupy a material space distinct from 'DNA nanotechnology' and DNA origami. Over the past two decades SNAs have revolutionized gene regulation, drug delivery, gene therapy, and molecular diagnostics, and show promise for both antisense and RNAi therapy. We focus here on recent advances in the synthesis and application of SNAs in gene and drug delivery, diagnostics, and immunomodulation, as well as on the utility of nanoflakes as intracellular mRNA detection systems.

Spherical Nucleic Acids as Delivery Systems of Bioactive Molecules

Spherical nucleic acids (SNAs) are structures composed of chemically modified inorganic nanoparticles (NPs; e.g., gold nanoparticles, AuNPs) at the core, and a dense layer of highly arranged thiol-modified oligonucleotides as the shell – which are chemically bound to the surface of the core via thiol bonds. Initially introduced by Mirkin and coworkers in 1996 [1], the advantages of SNA NPs include; (i) highly specific molecular recognition via specific Watson–Crick base-pairing, (ii) grafted oligonucleotides provide negative charge and increased colloidal stability as well as steric stabilization in solutions of elevated ionic strength, and (iii) the ability to couple with other biomolecules for molecular imaging or drug delivery [2]. NPs are an emerging class of intracellular delivery systems for bioactive molecules, and are promising carriers for antisense-based therapeutics and immunomodulators (see [Glossary](#)) in the absence of off-target effects, immunogenicity, or apparent cell toxicity [3]. A variety of single-stranded (ss) and double-stranded (ds) oligonucleotides, such as DNA, RNA, peptide nucleic acid (PNA), miRNA, small interfering RNA (siRNA), and locked nucleic acid (LNA), typically 25–40 nt and 7–12 nm in length, have been conjugated to the core to generate the NP shell [4–7]. Whole-transcriptome profiling of HeLa cells showed no significant up- or downregulation of genes in SNA-treated cells [8].

SNAs elicit a minimal immune response relative to cationic nanocarriers (>25-fold reduced immune response) [9,10]. Because of the high density of oligonucleotides at the surface of SNAs, they are resistant to degradation by nucleases and have better stability compared with linear nucleic acids. Furthermore, the association of cations with SNAs screens the negative charges of neighboring oligonucleotide strands and inhibits the activity of nucleases [11,12].

Unlike linear DNA, SNAs can enter cells without the assistance of transfection reagents. Although SNAs have a negative charge as a result of the high density of oligonucleotides (zeta potential of <30 mV), they can be recognized by class A scavenger receptors by their 3D structure, and are rapidly internalized by the caveolin endocytotic process in almost all cell types [13,14]. Interactions between DNA–AuNPs and these receptors seem to depend on the high density of oligonucleotides at the NP surface. When systemically administered, SNAs can cross the blood–brain barrier (BBB) and can traverse the epidermal barrier in C57BL/6 mouse models when applied topically [10,14]. In this review we discuss recent advances in the synthesis and properties of SNA NPs, their utility in the measurement of intracellular genetic material, for gene or drug delivery, and as potent gene regulation agents.

Synthesis and Properties of SNAs

The Core of SNAs

The properties of SNAs depend on the type of NP core used as the framework for assembling and arranging nucleic acids into a packed layer on the surface. A wide range of NPs including AuNPs,

Highlights

Nanotechnology provides new approaches for cancer therapy via the delivery of anticancer drugs using nanoparticles (NPs), by more sensitive diagnosis of cancer biomarkers and cancer cells, and by monitoring therapeutic efficacy and tumor burden over time.

The recent evolution of NP synthesis and functionalization allows targeted delivery of anticancer drugs to tumor sites with minimal cellular damage or side effects on healthy tissues and organs.

SNAs are an emerging class of intracellular delivery systems for the delivery of bioactive molecules, such as drugs and antisense-based therapeutics, and they are efficient for monitoring mRNA levels in living cells.

¹Immunology Research Center, Tabriz University of Medical Sciences, Tabriz, Iran

²Department of Biotechnology, Higher Education Institute of Rab-Rashid, Tabriz, Iran

³Department of Dermatology and Cutaneous Biology, Sidney Kimmel Medical College, and Jefferson Institute of Molecular Medicine, Thomas Jefferson University, Philadelphia, PA, USA

⁴Genetics, Genomics, and Cancer Biology PhD Program, Thomas Jefferson University, Philadelphia, PA, USA

⁵Research Center of Advanced Technologies in Medicine, Torbat Heydariyeh University of Medical Sciences, Torbat Heydariyeh, Iran

*Correspondence:
Behzad_im@yahoo.com,
Jouni.Uitto@jefferson.edu



quantum dots (QDs), SiO_2 , Ag, Fe_3O_4 , [PLGA (polylactic-co-glycolic acid)], proteins, liposomes, and platinum have been used as the SNA core [1,15–20]. At present, the most commonly used SNAs for biomedical applications employ a 10–15 nm Au core with thiol-linked nucleic acids [21,22] (Figure 1).

Most importantly, the shape and size of the NPs determine the maximum density of oligonucleotides at the particle surface. A spherical AuNP 10 nm in diameter supports $\sim 2.0 \times 10^{13}$ oligonucleotides per cm^2 , whereas under identical conditions $\sim 5.8 \times 10^{12}$ oligonucleotides/ cm^2 cover the surface of a planar AuNP [23]. Size is also important for spherical NPs because smaller NPs support higher densities of oligonucleotides owing to their higher radius of curvature, and this confers a natural deflection angle between nearby oligonucleotides that creates additional space around individual strands. This is crucial because increased oligonucleotide loading onto the core particle typically promotes SNA entry into cells [24].

AuNPs were initially chosen for the core material because they are easily synthesized over a range of particle diameters, display **plasmon resonance** with high extinction coefficients, can be easily functionalized with a wide variety of chemical reagents, and exhibit well-defined catalytic properties.

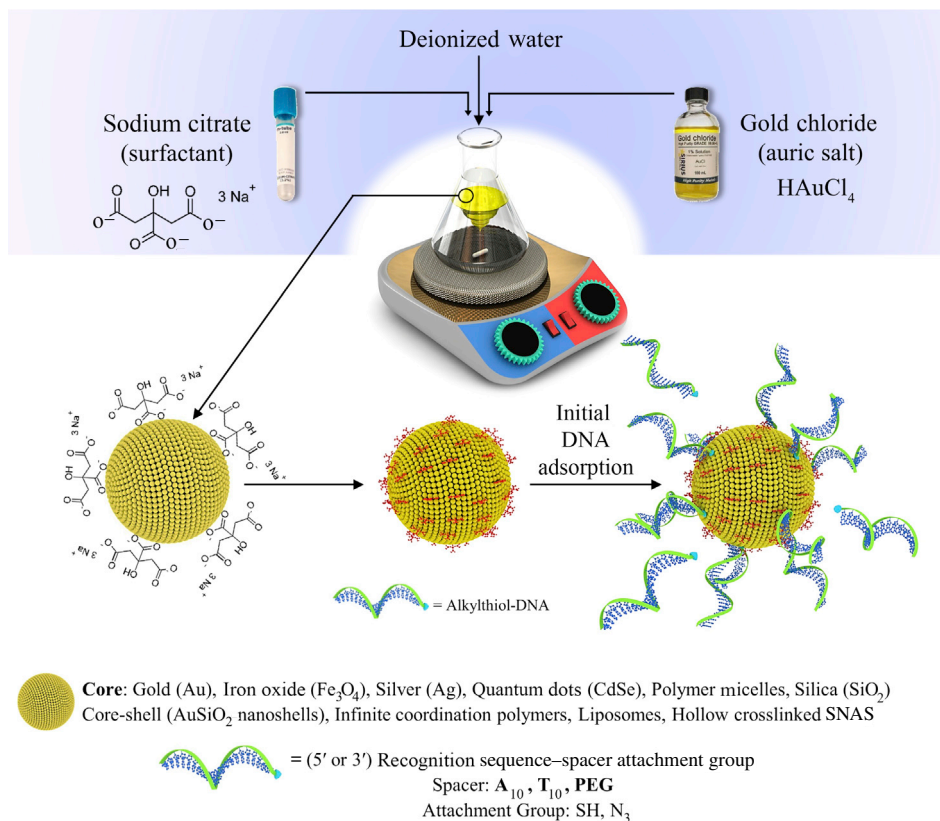


Figure 1. Spherical Nucleic Acid (SNA) Synthesis.

Citrate ions (upper left) are used to reduce chloroauric acid (HAuCl_4 ; upper right) to prepare uniform gold colloids. Citrate ions act as both capping and reducing agents. By mixing alkylthiol-modified nucleic acids with the solutions of citrate-capped gold particles, thiolated oligonucleotides are absorbed onto the surface of gold nanoparticles (AuNPs) and create a dense oligonucleotide shell (lower left). Alkyl thiol or cyclic disulfide chemical tethering groups are used to conjugate the oligonucleotides to the surface of AuNPs. A base sequence (~ 15 –25 nt) acts as a recognition segment that is complementary to the target sequence, and a further 10 nt sequence acts as a spacer between the NP surface and the recognition element. Abbreviation: PEG, polyethylene glycol.

Glossary

Cancer gene therapy: specific delivery of genetic material into a cancer cell to restore the function of damaged genes, to induce apoptosis, or to restore aberrant signaling pathways.

Frens method: a simple method for the production of monodisperse spherical gold nanoparticles (AuNPs) suspended in water with a diameter of 10–20 nm.

Immunomodulator: a chemical agent which changes the immune response or function of the immune system.

Nanoflares: comprise a monolayer shell of ssDNA complementary to a target mRNA on the surface of spherical AuNPs. The recognition sequences are attached to the AuNP via a 3' thiol group. The ssDNA recognition sequence is prehybridized with a reporter flare sequence that contains a fluorophore whose fluorescence is quenched in proximity to the AuNP.

Nanoparticle opsonization: the removal of NPs coated with opsonin proteins from the circulation by immune system cells. Opsonin proteins attached to the NP surface make them more visible to phagocytic cells.

Nanoparticle PEGylation: PEG moieties constitute an inert polymer that can inhibit NP interactions with blood components and thus reduce opsonization, aggregation, and phagocytosis of NPs by the reticuloendothelial system (RES), thereby prolonging their circulation time.

Plasmon resonance: a prominent spectroscopic feature of noble metal NPs which generates a sharp and intense absorption band in the visible range.

Protein corona: after intravenous administration of NPs, blood components adsorb to the NP surface, generating a protein-rich layer, the corona, on the surface of NPs.

Quantum dots (QDs): small semiconductor NPs that are used as biological labels. Larger QDs (diameter 5–6 nm) emit longer wavelengths, resulting in emission colors such as orange or red. Smaller QDs (diameter 2–3 nm) emit shorter wavelengths,

Different techniques, such as the **Frens method**, can be used for the synthesis of the SNA core. Typically, citrate ions are employed to reduce chloroauric acid (HAuCl_4) to generate uniform Au colloids 5–150 nm in diameter, and citrate ions act as both capping and reducing agents [25] (Figure 1). A high-density SNA shell is then prepared in an aqueous solution at high salt concentration (usually 0.15–1.0 M) [23].

Although AuNPs are most commonly used for generating SNAs, the recent introduction of biodegradable and biocompatible nanostructures, such as liposomes, proteins, and PLGAs, has opened exciting new avenues for controllable drug delivery systems, and for long-term oligonucleotide release to regulate intracellular biological processes [26].

Attaching Nucleic Acids to the Core

Nucleic acids for attachment to the core comprise three distinct segments; (i) an alkyl thiol anchor that is used for conjugation to the AuNP surface, most commonly a hexamethylene linker [$-(\text{CH}_2)_6-$] or cyclic disulfide chemical tethering group, (ii) a spacer arm of ~ 3 nm: oligoethylene glycol (OEG) or poly-adenine (poly-A) (10 nt) are most commonly used as spacers between the NP surface and the recognition element, and the spacing promotes effective interactions between the recognition element and the target sequence [23,27], and (iii) the oligonucleotide recognition segment, a 15–25 nt sequence complementary to the target sequence.

By mixing alkyl-thiol-modified nucleic acids with solutions of citrate-capped AuNPs, thiolated oligonucleotides are adsorbed onto the surface of the AuNP, creating a dense oligonucleotide shell because of the high affinity of thiol moieties for AuNPs. The negative charge of the oligonucleotide backbones can be counterbalanced by adding monovalent counterions (such as Na^+) to facilitate dense NP formation (Box 1). In fact, a higher concentration of NaCl in the reaction solution enhances this screening and increases the number of nucleic acid strands per NP.

Although nonthiolated oligonucleotide strands can be attached via nitrogen–Au coordination to AuNPs to form functional SNAs, most SNAs are prepared by binding thiolated oligonucleotides to the surface of AuNPs [2,24]. At neutral pH, both citrate-capped AuNPs and oligonucleotide strands are negatively charged; therefore, if citrate-capped AuNPs are simply mixed with thiolated oligonucleotides, electrostatic repulsion results in slow adsorption of oligonucleotides onto the AuNP surface and low loading capacity. Accordingly, it is necessary to reduce the electrostatic repulsion between the NP surface and DNA [2]. Two methods are currently applied to achieve this goal. The first is to add an electrolyte (e.g., NaCl) to the solution to reduce the electrostatic repulsion between the AuNPs and oligonucleotides [2,28,29]. In another effective approach, reducing the pH of the solution assists DNA adsorption onto the AuNP surface, but there are concerns regarding nonspecific adsorption.

Recently, Sun and coworkers compared the efficiency of these two methods (low-pH protocol and the salt-aging method) for preparing SNA NPs [2]. Their results showed that both methods were similar in terms of the average binding affinity of each thiolated oligonucleotide probe to its complementary

resulting in colors such as blue and green.

Scanometric miRNA (scano-miR) array profiling assay: a miRNA profiling method that is amenable to massive multiplexing for screening samples down to 1 fM concentrations for thousands of short miRNA targets, and can distinguish perfect miRNA sequences from those containing a SNP.

Small unilamellar vesicles (SUVs): spherical vesicles up to 100 nm in diameter that comprise a single amphiphilic lipid bilayer enclosing an aqueous solution.

Survivin: an antiapoptotic protein which inhibits the activation of caspases. Survivins are overexpressed in most tumor cells.

Vroman effect: the adsorption of blood serum proteins to the surface of NPs in the bloodstream.

Zeta potential: a measure of the effective electric charge on the NP surface. The magnitude of the zeta potential provides information about particle stability. NPs with a higher-magnitude zeta potential exhibit increased stability because of larger electrostatic repulsion between particles.

Box 1. The Role of Metal Ions in Controlling the Properties of SNAs

Although several different methods are used for the synthesis and assembly of SNAs, the metal concentration and the type of ion in solution play a vital role in controlling the properties of SNAs. Typically, to reduce the negative charge of SNAs, sodium ions (Na^+) are used to stabilize the SNA assemblies. In comparison with monovalent ions, the higher charge of divalent metal ions (M^{2+}) creates a stronger stabilizing effect on DNA duplex formation [83]. Recently, Joo and Lee investigated the interaction of various divalent metal ions (Zn^{2+} , Co^{2+} , Cd^{2+} , Mn^{2+} , Cu^{2+} , and Ni^{2+}) with SNAs and their effects on the structure and properties of gold SNAs. Their results showed that the assembly properties of SNAs are most strongly affected by cupric ions (Cu^{2+}) in relation to M^{2+} -mediated DNA bonding [83].

strand, as well as the number of complementary oligonucleotides bound to each SNA, although a higher loading capacity was observed with the low-pH protocol. Furthermore, nonspecific oligonucleotide binding could be prevented almost completely simply by treating the SNAs with glutathione (GSH) [2].

Uptake of SNAs

Delivery of negatively charged oligonucleotides to target cells usually requires viral or non-viral delivery systems. Viral vectors offer better efficiency for gene delivery but suffer from fundamental drawbacks such as random insertional mutagenesis, limited capacity, immunogenicity, tumorigenicity, and a high cost of large-scale production. Classical non-viral gene carriers such as cationic polymers, cationic liposomes, and peptides can have off-target effects because their positive charge can alter nontarget gene expression. Unlike linear oligonucleotides, SNAs are rapidly internalized into different cell lines without complexing with a carrier. In fact, the delivery of negatively charged oligonucleotides into cells requires a positively charged carrier for nucleic acid condensation, and this is usually cytotoxic owing to its positive charge. However, if the oligonucleotides are densely packed at the nanoscale, as in the case of SNAs, they enter cells in high numbers and are resistant to degradation by nucleases, show no apparent toxicity, and do not activate an innate immune response.

Another important difference between SNAs and linear oligonucleotides is that SNAs are dense spherical arrays of short nucleic acids in a defined orientation on the 3D scaffold of the core, whereas the general shape of oligonucleotides is usually determined by the hybridized duplex structural unit [14]. Furthermore, relative to free nucleic acids of the same sequence, SNAs show a >100-fold higher binding capacity for free complementary nucleic acids [30]. The oligonucleotide array also confers well-defined catalytic properties in addition to specific physical and chemical properties such as plasmon resonance with high extinction coefficient, light scattering, and quenching [31].

In addition to the choice of the core material, efficient cellular SNA uptake is influenced by several parameters including; (i) the sequence of the oligonucleotide strands, (ii) the morphology of the strands, (iii) the loading density, (iv) the sugar backbone, and (v) the size of the NPs (Box 2) [27,32].

SNA Interactions with Serum Proteins

There are more than 1000 different proteins and lipids in plasma, and these compete for adsorption to the NP surface [33,34]. Adsorption affinity between blood serum proteins and the NP surface, the so-called **Vroman effect**, is affected by the available surface as well as by the affinities, abundance, and incubation time of NPs with these proteins [35,36]. After intravenous administration of NPs, blood and its components are the first barriers to the activity of NPs because they generate a protein-rich layer at the surface of NPs, referred to as a **protein corona**.

Initially, the most abundant proteins adsorb to the surface of NPs, but over time these proteins are replaced by high-affinity proteins [34]. After only 30 s of interaction of NPs with human plasma, nearly

Box 2. Effects of the Sugar Backbone on Cellular Uptake of SNA NPs

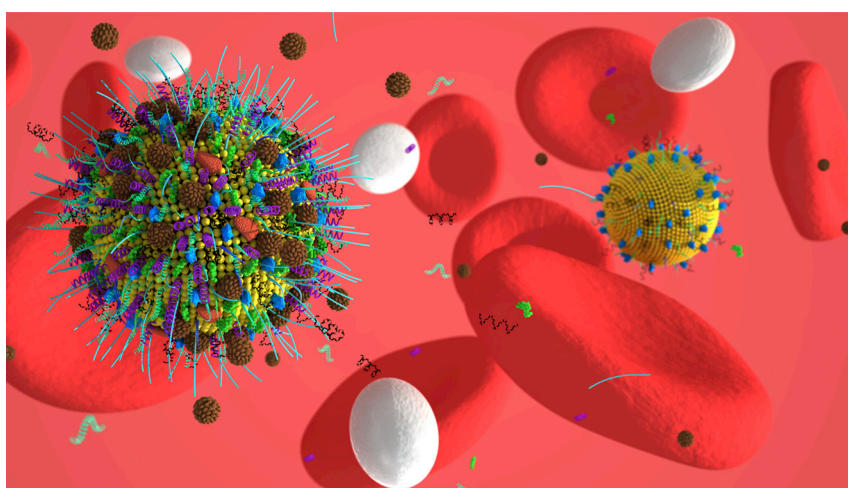
Modification of the oligonucleotide sugar backbone can influence the surface chemistry, lipophilicity, and hydrogen bonding interactions of SNAs, and therefore affect their cellular uptake properties. Song *et al.* recently investigated five different sugar backbones, namely DNA, RNA, L-DNA, 2'-fluoroRNA (2'-F-RNA), and 2'-methoxy-RNA (2'-OMe-RNA) for their effects on cellular uptake [32]. Both uptake mechanism and efficiency significantly depended on the type of backbone. To examine the pathways of endocytosis, cells were treated with SNAs in the absence or presence of different endocytosis pathway inhibitors. Among the tested backbones, SNAs with the 2'-F-RNA modification showed the highest cellular uptake level owing to increased lipophilicity [SNA-2'-F-RNA (222%) > SNA-RNA (147%) > SNA-DNA (100%) > SNA-L-DNA (60%) > SNA-2'-OMe-RNA (41%)] (Figure S1) [32]. All modified SNAs exploited scavenger receptor-mediated endocytosis as the main internalization mechanism.

300 proteins are bound to the surface of NPs, and longer exposure times enhance the total protein absorption [37,38]. The corona layer can be divided into a hard corona (HC) and a peripheral soft corona (SC). The HC is strongly attached to the NP surface and contains proteins with high affinity for NPs, whereas the SC exhibits dynamic exchanges and comprises proteins that only interact with NPs with low affinity [39,40]. The SC interacts with the HC via weak protein–protein interactions, is exchangeable over time, and can be easily removed by washing steps [41]. The structure and composition of the corona proteins are related to the physicochemical properties of the NPs, including surface functional groups, shape, size, charge, and composition, as well as the physiological environment of the NPs, including blood, biological fluids, the duration of exposure, and the bio-reactivity of the NPs [41]. Therefore, the interaction between NPs and the protein corona may change the size, charge, and interface composition of NPs as well as their functionality by conferring a new biological character that can be recognized by cells. Their biological identity can determine the physiological response, including accumulation, toxicity, cellular uptake, agglomeration, circulation half-life, kinetics, signaling, and transport [34,39]. The size of the NPs is an important factor governing the nature of the corona [39] because larger NPs proteins may stretch over NPs to adapt to their surface, whereas smaller NPs demonstrate reduced interactions with proteins [37,42].

NP uptake occurs through a two-step process in which NPs adhere to the plasma membrane and are subsequently internalized to the cell via different pathways [43,44]. Interaction of NPs with the protein corona dramatically decreases NP adhesion to cell membranes and can have a major impact on drug release [44]. It should be noted that the protein corona significantly alters the *in vivo* behavior not only of SNAs but also of all types of NPs; however, protein corona effects can be modulated by SNA design (Figure 2) [45].

Nucleic Acid Structure Affects the Formation of the Protein Corona

To investigate the effect of 3D nucleic acid structure on the formation of the protein corona around the SNA surface, Chinen *et al.* studied the type and number of proteins binding to SNAs as a function of the DNA sequence [45]. Because G-quadruplexes (four-stranded nucleic acid secondary structures which form between guanine-rich sequences) are recognized and bind better to class A scavenger receptors than do ssDNA molecules [46], studies have focused on G-rich sequences in oligonucleotides that play an important role in SNA cellular internalization through interactions with scavenger



Trends in Molecular Medicine

Figure 2. Interaction of Spherical Nucleic Acids (SNAs) with the Protein Corona in the Bloodstream.

After intravenous administration of SNAs (left), nanoparticles encounter a large mass of proteins in the serum and a corona layer is generated around the SNAs (right; shown as adsorbed green, blue, and cyan globules), which significantly alter its size and *in vivo* behavior, thus limiting the application of SNAs.

receptors [45,47]. Binding to cell-surface scavenger receptors depends on the sequence of the SNA nucleic acid, and nucleic acid tertiary structures can significantly change the surface chemistry of SNAs [47]. In addition, although the protein corona generally decreases NP adhesion to cell membranes, corona proteins may enhance SNA uptake by macrophages, leading to their accumulation in the liver and spleen after intravenous administration [48].

Effect of PEGylation on the Activity of SNAs

To deliver adequate concentrations of bioactive components via systemically administered therapeutics, and to reach the desired target, NPs must circulate in the bloodstream for an extended period of time. Therefore, NPs must bypass different barriers that cause fast clearance of NPs, including; (i) **nanoparticle opsonization** or agglutination because of their interaction with serum proteins, and (ii) the reticuloendothelial system (RES) that antagonizes NP action because it clears NPs from the circulation [49] and thus inhibits site-specific accumulation of NPs at target sites. To increase the half-life of NPs in the circulation, the interaction of NPs with blood components needs to be reduced. One approach is to coat the surface of NPs with an inert polymer such as polyethylene glycol (PEG) to impart 'stealth' properties [50]. Coating of NP surface with PEG shields the surface from opsonization, aggregation, and phagocytosis by the RES, and thereby prolongs NP half-life in the circulation. PEGylation has been classified as 'generally regarded as safe' (GRAS) by the FDA, and has a long history of safe application in humans [51]. Thus, PEGylation of NPs is a promising strategy to prolong their circulation time.

There is an abundance of information about the effects of **nanoparticle PEGylation** on the structural properties and biological activity of SNAs. Chinen *et al.* evaluated the effect of PEGylation (PEG-thiol) on the functional activity of RNA-SNAs [52]. They used two methods: the backfill approach and coadsorption methods (Figure S2 in the supplemental information online). In the backfill approach, a 200-fold excess of thiolated duplex siRNAs was first adsorbed onto the surface of AuNPs with a diameter of 13 nm and, after 4 h of incubation, a 2000-fold excess of alkanethiol-modified PEG was added [53]. The results showed that the length of PEG thiol (2 kDa) that spread out from the RNA duplexes on the SNA NP surface increased the particle size from 34 ± 1 to 41 ± 1 nm. In addition, adsorption of PEG groups to the SNA surface affected the surface charge, and changed their zeta potential from -33 ± 1 to -29 ± 2 mV because of PEG-mediated shielding of the negatively charged RNAs at the surface of the SNA. In coadsorption methods, alkanethiol-modified RNA duplexes and PEG-alkanethiols coadsorbed onto the surface of 13 nm AuNPs at different ratios. The number of RNA strands loaded per AuNP increased when AuNPs were incubated with a higher RNA:PEG molar ratio. Collectively, the results showed that, in comparison with the backfill method, coadsorption of siRNA and PEG onto the surface of AuNPs increases the number of PEG and RNA molecules that can be loaded onto the SNA surface. Thus, the second approach proved to be more efficient for preparing PEGylated SNAs with more controllable PEG content. This method is used as a primary synthetic approach for systematically controlling RNA-SNAs and PEG-loading effects. Furthermore, studies on the impact of PEGylation on the biological fate of RNA-SNAs showed that increasing PEG loading on SNAs led to reduced SNA corona formation, and thus to an enhanced blood circulation half-life of SNAs. However, increasing PEG density on the surface of RNA-SNAs may decrease interactions of PEG-RNA-SNAs with class A scavenger receptors, leading to reduced cellular uptake by target cells [53].

Liposome-Based SNAs

The most widely studied conjugates so far have consisted of AuNP cores functionalized with oligonucleotides alkylthiolated at the 3' or 5' end of the molecule, that are attached to the NP through an Au-S bond. Recently, a novel class of metal-free SNA nanostructures was synthesized by Banga *et al.* [54] using liposomes as the core. Conventional liposomes are closed spherical vesicles with at least one lipid bilayer and contain a core aqueous solution that can be used as a carrier for the administration of nutrients or drugs. Unlike conventional liposome structures, the SNA carrying liposomes were assembled with an oligonucleotide cargo at the liposome surface. Two steps are necessary to synthesize typical liposomal SNAs: first, 30 nm diameter **small unilamellar vesicles (SUVs)** are prepared from lipid monomers; next, the surface of the liposomes is functionalized by an oligonucleotide derivative possessing a hydrophobic tocopherol moiety, which can effectively intercalate into the phospholipid bilayer of SUVs via hydrophobic interactions (in the ratio of 80:1 of lipid to nucleic acid) (Figure S3) [54]. Studies on the effects of anti-HER2 liposomal

SNAs on SKOV-3 cells have shown that liposomal SNAs can effectively knockdown *HER2* gene mRNA in these cells [54]. Zhang *et al.* further introduced a biodegradable and biocompatible DNA-brush block copolymer (DBBC) for liposomal SNAs, which showed the natural cellular uptake properties of conventional SNAs with inorganic cores. DBBC-based micelle SNAs show a more negatively charged surface, a greater surface mass of oligonucleotides, a cooperative melting profile, a higher melting temperature, and a high cellular uptake efficiency compared with micelle SNAs constructed from linear block copolymers. It is important to note that, under physiological conditions, these polymer-based SNAs can be steadily degraded via acid-catalyzed or esterase-catalyzed cleavage of ester bonds, resulting in slow release of the payload nucleic acid [16].

Application of SNAs in Gene Regulation

Current cancer gene therapies rely on delivery of genetic material into a host cell via viral or non-viral vectors to restore the function of damaged genes or signaling pathways, induce apoptosis, or inhibit oncogenes [55]. Gene delivery can also be used to manipulate the tumor microenvironment or stimulate the host immune system against cancer cells, for example, by antisense oligomer delivery [52,56] (Box 3). One major obstacle to successful gene delivery is the lack of safe and clinically effective delivery systems. Owing to the negative charge of nucleic acids, they are repelled by negatively charged plasma membranes and cannot easily cross them [55,57]. In addition, they are rapidly degraded by nucleases, and virus-based gene carriers may lead to stimulation of the innate immune response, accompanied by secretion of anti-inflammatory cytokines and chemokines around the site of administration. Furthermore, stimulation of a specific immune response, involving the production of antibodies by B lymphocytes and the activation of T lymphocytes, can occur after the introduction of vectors into the body [58,59]. For this reason, different non-viral carriers, including cationic lipids and polymers as well as biodegradable NPs, have been developed to shield them from enzymatic degradation and accelerate their internalization by target cells [57]. Unfortunately, most of these systemic delivery methods are not ideal because of their toxicity at high concentrations, low cellular uptake efficiencies, inability to be degraded naturally, and immune system stimulation when utilized for *in vivo* gene/drug delivery [1]. SNAs provide a new generation of nanocarriers for intracellular delivery of bioactive molecules (Table 1). Despite the substantial negative charge at the SNA surface, SNAs are able to enter various types of cells (>50 types of cell lines) at very high numbers without ancillary transfection agents [10]. Therefore, for both *in vitro* and *in vivo* applications, SNAs could be considered as a highly efficient vehicle for the regulation of gene expression through RNA interference (siRNA delivery) or antisense interactions with genes (antisense oligomer delivery) [18,60].

Delivery of siRNA and miRNA

In a recent study, Ruan *et al.* [60] introduced a so-called DNA nanoclew (DC), a metal- or cation-free SNA conjugate. In this new class of NPs, siRNA is attached to the surface of a DNA nanostructure as a core. The DNA nanostructure was synthesized by DNA rolling-circle amplification (RCA) to generate a clew-like

Box 3. Immunomodulatory Activity of SNAs

In cancer therapy, SNAs can be used as antigen carriers to selectively activate T cells. Nucleic acids can stimulate the immune system by binding to endosomal Toll-like receptors (TLR3, TLR7/8, and TLR9) [84,85]. Recently, several studies investigated the immunomodulatory activities of SNAs [86–88]. Radovic-Moreno *et al.* designed an immunomodulatory SNA system which could be used for regulating (immunoregulatory, IR-SNA) or stimulating (immunostimulatory, IS-SNA) immune responses by engaging TLRs [86]. IR-SNAs consisted of a shell of TLR antagonist oligonucleotides, whereas IS-SNAs contained a shell of TLR agonist oligonucleotides. In comparison with the corresponding free oligonucleotides, IS-SNAs resulted in up to 700-fold higher IgG2a serum titers, 400-fold higher cellular responses, and 80-fold increased inhibition of RAW 264.7 macrophages, and improved treatment of mice with lymphomas. Conversely, IR-SNAs revealed an up to a 70% reduction of fibrosis score and eightfold increase in potency in mice with nonalcoholic steatohepatitis (NASH) [86]. Given the potential of SNAs for clinical applications in view of their potency, defined chemical nature, sequence-specific TLR activation, and good tolerability, SNAs are attractive new modalities for immunotherapy.

Table 1. Applications of SNAs as Carriers in Delivery Systems

Drug/target	Disease model	Cell line tested	Assayed genes	Assay conditions	Refs
miR-34a	Breast cancer	MCF-7	<i>Survivin</i>	<i>In vitro</i>	[67]
miR-99b	Sepsis	RAW264.7	<i>MFGE8</i>	<i>In vitro/in vivo</i>	[69]
miR-182	Glioblastoma	LN229, LN2308, U87MG	<i>BCL2L12</i>	<i>In vitro/in vivo</i>	[89]
miR-21	Prostate cancer	PC-3	<i>miR-21, PTEN</i>	<i>In vitro</i>	[70]
miR-182	Glioblastoma	U87MG	<i>BCL2L12, c-MET, HIF2A</i>	<i>In vitro/in vivo</i>	[90]
lncRNAs (long noncoding RNAs)	Adenocarcinoma	A549	<i>IFIT2, MALAT1</i>	<i>In vitro</i>	[91]
siRNA	Diabetes	Primary mouse keratinocytes	<i>Gm3s, Igf1r, Egfr</i>	<i>In vitro/in vivo</i>	[92]
siRNA	Psoriasis	A431	<i>EGFR, EGF</i>	<i>In vitro/in vivo</i>	[93]
siRNA	Glioblastoma	U87MG, SF767, GIC-20	<i>MGMT, caspase 3, caspase 7</i>	<i>In vitro/in vivo/ex vivo</i>	[63]
Ribozymes	Glioblastoma		<i>MGMT</i>	<i>In vitro</i>	[7]
siRNA	Prostate cancer	LNCaP	<i>Androgen receptor</i>	<i>In vitro</i>	[94]
siRNA	Skin disease	Human epidermal keratinocytes, HeLa, HaCaT	<i>EGFR, ERK</i>	<i>In vitro/in vivo</i>	[10]
siRNA	–	HeLa, Jurkat, MCF-7	<i>Actin, survivin</i>	<i>In vitro</i>	[75]
siRNA	Glioblastoma	U87MG, huTNS, LN235, LN2308	<i>BCL2L12, caspase 3, caspase 7</i>	<i>In vitro/in vivo</i>	[95]
siRNA	Glioblastoma	U87MG	<i>GLI1</i>	<i>In vitro</i>	[38]
siRNA	Glioblastoma	U87MG	<i>GFP</i>	<i>In vitro</i>	[18]
Paclitaxel	Ovarian cancer	SKOV-3	<i>BCL2</i>	<i>In vitro</i>	[72]
Platinum (Pt)	Cervical cancer Lung cancer	HeLa, A549	–	<i>In vitro</i>	[96]
Paclitaxel	Breast adenocarcinoma Ovarian cancer Uterine sarcoma	MCF7, SKOV-3, MES-SA/Dx5	–	<i>In vitro</i>	[97]
Doxorubicin	Ovarian cancer	SKOV3	–	<i>In vitro</i>	[74]
Camptothecin	–	A549, NIH 3T3, C166, HaCaT	–	<i>In vitro</i>	[98]
TMPyP4	–	SKOV3, HBE135	–	<i>In vitro</i>	[68]
Doxorubicin	Cervical cancer	HeLa	–	<i>In vitro</i>	[99]

shape. Then, numerous copies of siRNA duplexes were grafted onto the structure, exploiting the complementary overhang sequence of the linear DC template, and base-pair hybridization thus generates a new type of SNA NP, termed a DC-siRNA. The DC-siRNA NPs are internalized via class A scavenger receptor-mediated endocytosis, and the endogenous Dicer enzyme subsequently cleaves the siRNA, releasing it from the DC and allowing targeted siRNA-mediated gene silencing. *In vitro* experiments verified that such SNAs led to potent gene knockdown with negligible cytotoxicity [60].

In a recent study, Sita *et al.* [63] introduced a new SNA as a BBB- and blood–tumor barrier (BTB)-penetrating nanostructure for the delivery of siRNA and miRNA to intracranial glioblastoma (GBM) tumor sites to knock down O⁶-methylguanine-DNA-methyltransferase (MGMT). A single intravascular

administration of MGMT-targeting siRNA-SNAs elicited intratumoral MGMT protein knockdown *in vivo* [63]. Overall, the efficiency of this new class of SNAs for siRNA delivery is comparable with traditional transfection reagents, such as polymeric materials and liposomes. For example, the tumor-suppressor miR-34a, which is downregulated in different types of cancers [64], including lung [65], breast [61], and colon cancer [62], has functions in cell migration and proliferation, drug resistance, and invasion [62,66]. To deliver miR-34a to MCF-7 breast cancer cells, Li *et al.* used SNAs as carriers and were able to induce apoptosis and reduce the viability of these cells *in vitro* [67]. For oncogenic miRNA, their activity can be inhibited by antagomirs that bind to complementary sequences in the target miRNA and function as a miRNA sponge. Wang *et al.* [69] used SNAs as carriers for delivery of anti-miR-99b into a macrophage cell line to enhance the expression of MFG8, that is known to play a significant role in the survival and maintenance of intestinal epithelial homeostasis, including restitution and migration. Owing to the high efficacy of oligonucleotide delivery via SNAs, a lower effective dose is needed compared with treatment with free antagomirs. Their results showed that the SNA delivery of anti-miR99b could rescue *MFG8* gene expression and maintain intestinal epithelial homeostasis in sepsis [69]. Overall, these studies demonstrate that SNAs provide a promising approach to deliver siRNA or RNA sponges.

Delivery of SNAs by Exosomes

Exosomes are promising endogenous nanocarriers for delivering therapeutic RNAs to specific tissues within living organisms. The potential of loading and delivery of SNAs by exosomes has been investigated by Alhasan *et al.* [70] using SNAs as carriers for anti-miR-21. Transmission electron microscopy (TEM) analyses revealed that PC-3 cells effectively endocytosed the SNA constructs and stored a small portion of them (<1%) in exosomes. The exosome-wrapped SNAs could be secreted into the surrounding extracellular fluid and then be selectively reintroduced into the cells. Delivery of anti-miR21 using these SNAs showed a ~50% reduction of miR-21. A ~3000-fold higher concentration of anti-miR21 SNAs is necessary for similar knockdown of miR-21 by free SNAs (without exosomes). These results showed that exosomal entrapment by the natural cellular machinery could be a promising method to enhance the effectiveness of SNAs [70].

Application of SNAs in Drug Delivery

A new SNA-based delivery system for the class I phosphoinositide 3-kinase (PI3K) inhibitor buparlisib (BKM120), an anticancer drug, was introduced by Bousmail *et al.* for the treatment of chronic lymphocytic leukemia (CLL) [71]. BKM120 can cross the BBB, resulting in toxicity in the central nervous system (CNS), thus hindering its potential use [71]. To reduce these off-target effects, Bousmail *et al.* developed a DNA NP platform for the delivery of BKM120. For the construction of this nanostructure, 19-mer DNA strand units were built on a glass pore support followed by the addition of dodecane monomers (hexaethylene, HE) to produce a monodisperse HE12–DNA conjugate. After preparation of BKM120-loaded HE12-SNAs in the presence of BKM120, self-assembly of the polymer–DNA conjugates and subsequent purification resulted in nearly monodispersed HE12-SNAs. These BKM120-loaded NPs could be efficiently taken up by HeLa cells, induce apoptosis in CLL lymphocytes, and act as sensitizers for other antitumor drugs, such as doxorubicin (Dox), without eliciting inflammation. Investigation of the interaction of these NPs with corona proteins showed that there was no interaction with human serum albumin, and therefore the NP may possibly avoid RES-mediated uptake. Biodistribution studies on this drug delivery system showed long circulation times (up to 24 h), full body distribution, minimal leakage through the BBB, and high accumulation at tumor sites in xenograft models. The results demonstrated that these delivery vehicles have great potential as a general platform for chemotherapeutic drug delivery [71].

Tan *et al.* investigated SNA NPs for the delivery of paclitaxel into SKOV-3 cells [72]. Their DNA–paclitaxel nanostructures were effectively internalized to target cells, exhibited stability against nucleases, and showed nearly identical cytotoxicity to the free drug. Zheng *et al.* used AS1411 aptamer SNAs for the delivery of Dox and TMPyP4 (a photodynamic therapy drug) into SKOV-3 cells [68]. AS1411 binds to TMPyP4, and can specifically target nucleolin, a protein overexpressed in many tumor cells, thus enabling cell-specific targeting by these multimodal SNAs. Flow cytometry results demonstrated a marked change in the fluorescence signal shift induced by AS1411 SNAs in nucleolin-expressing SKOV-3 cells. Furthermore,

studies on cell death following laser irradiation showed that TMPyP4/AS1411 SNAs exhibited significantly higher phototoxicity than pure TMPyP4 [68].

In another study, Banga *et al.* developed Dox-loaded polymeric SNAs (Dox-PSNAs) to target SKOV-3 ovarian cancer cells. The dense layer of nucleic acid on the surface of these SNAs resulted in greater cellular uptake of Dox-PSNAs and manifested a comparable level of cytotoxicity with free Dox [74].

Taken together, these studies demonstrate that SNAs provide a means to control the release of the encapsulated payload, and constitute a promising platform for chemotherapeutic drug delivery, thereby opening new avenues for cancer therapy.

Intracellular and Intercellular Tracking of miRNAs by Nanoflares

In addition to the use of SNAs for the delivery of antisense oligonucleotides, NPs can be used as probes for measuring genetic material in cells and blood. Recently, **nanoflares** have been introduced as new SNA nanoconstructs to detect intracellular mRNA levels as well as a means of scar diagnosis without biopsy [73,75,76]. Nanoflares are generated using a recognition sequence containing a 3' thiol and consist of a monolayer shell of ssDNA complementary to the target mRNA. The ssDNA recognition sequence is prehybridized with a reporter flare sequence whose fluorescence is quenched in proximity to the AuNP. Binding of the recognition sequence to the target mRNA results in displacement of the reporter flare strand, thus generating a fluorescent signal (Figure 3) [77,78]. Prigodich *et al.* developed a multiplexed nanoflare for the detection of **survivin** levels in HeLa, Jurkat, and MCF-7 cells [75]. For the synthesis of SNAs, they used citrate-capped 13 nm AuNPs and alkylthiol-modified target DNA strands. In the presence of survivin as the target gene, fluorescence increased at wavelengths corresponding to the survivin flare [75].

To detect low-abundance miRNAs in serum, cancer cells, and tissue samples, Alhasan and coworkers introduced a new **scano-miR (scano-miR) array profiling assay** [79]. In this method, target miRNAs are ligated to a DNA sequence as a linker. The chimeric miRNA–DNA structures, when added to a commercial miRNA array where the miRNA sequences hybridize to complementary DNA, are captured at specific spots on the array. At these spots, the DNA linkers interact with AuNPs modified with oligonucleotides that contain the complementary sequence. After washing the samples, the miRNA array is treated with tetrachloroaurate and hydroxylamine, leading to deposition of Au⁰ (reduced Au) on the immobilized AuNPs. This procedure enhances the light-scattering

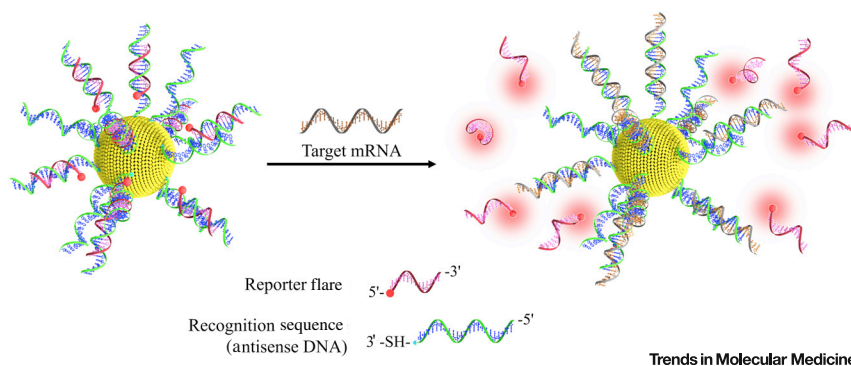


Figure 3. NanoFlare Structures and Their Application for the Detection of Target Molecules

Nanoflares are intracellular probes consisting of oligonucleotides immobilized on nanoparticles (NPs) that can recognize intracellular nucleic acids, thus releasing a fluorescent reporter dye. Generally, a single-stranded DNA (ssDNA, green/blue) complementary to the mRNA (brown) of the target gene is constructed containing a 3' thiol for binding to a gold NP. The ssDNA 'recognition sequence' is prehybridized to a shorter DNA complement containing a fluorescent dye (red) that is quenched. When the ssDNA recognizes its complementary target, the labeled strand is released from the complex, generating a fluorescence signal.

properties of AuNPs, allowing higher sensitivity and amplification of the signal that is read using a conventional scanner; the scano-miRNA system could detect miRNA at 1 fM concentration in serum with SNP mismatch specificity. The accuracy of this system for detecting deregulated miRNAs in prostate cancer is about 98.8% [79]. This simple, reproducible, powerful, and rapid scano-miR system allows simultaneous quantification of known miRNA sequences with minimal modification and purification steps. Therefore, this approach provides a sensitive and selective assay system that is an attractive alternative to current conventional methods (Figure S4) [79].

This approach has already been used to identify five miRNAs (miR-106a, miR-135a, miR-200c, miR-433, and miR-605) as prostate cancer markers in serum samples from prostate cancer patients [80]. The miRNA biomarker panels were able to differentiate, with at least 89% accuracy, between patients with low- and very high-risk forms of prostate cancer. Therefore, this system provides a simple diagnostic tool for prostate cancer without surgical intervention [80].

Metastatic cancer cells often spread to distant organ sites by adopting the epithelial–mesenchymal transition (EMT) developmental program, which involves upregulating vimentin and fibronectin, and cellular loss of epithelial markers such as E-cadherin. Therefore, nanoflares containing antisense recognition motifs for vimentin, twist, fibronectin, and E-cadherin were used to detect target mRNAs in a cell line model of metastatic breast cancer (MDA-MB-231). Most importantly, nanoflare technology allowed for the first time the detection and isolation of circulating tumor cells (CTCs) from human blood [81].

Overall, nanoflares can be used for the detection of different intracellular targets, such as altered mRNA levels, in cancer cells. Their advantages include high transfection efficiency, enzymatic stability, good optical properties, biocompatibility, and high selectivity and specificity. In the future, multiplexed assays and Förster resonance energy transfer (FRET)-based systems could be designed based on the ability of nanoflares to detect and analyze genetics-based diseases, such as most forms of cancers.

Concluding Remarks

SNAs represent an emerging class of nucleic acid constructs for application in research and clinical settings. Because of their high capacity to hybridize with complementary target sequences, SNAs have enormous potential in different areas of medicine, including molecular diagnostics and antisense gene therapy. They can enter essentially every known cell type in high quantities without using transfection agents, and they can cross the epidermis as well as the BTB and the BBB. Furthermore, SNAs are ideal candidates for systemic administration because they are resistant to nucleases and do not stimulate the immune system [11,12]. Moreover, SNAs have potential to be conjugated to different drugs, antibodies, or small molecules for use as multifunctional materials [59,60,82].

SNA-based nanoflares are ideal probes and offer tremendous potential for cancer research and in clinical settings, without adverse effects on cells. They are able to enter cells and detect target mRNAs with high sensitivity and selectivity. Future work should explore the potential of nanoflares for the detection and analysis of genetics-based diseases such as most forms of cancers (see Outstanding Questions). Oligonucleotides have potential to be customized for the diagnosis and treatment of many diseases, notably when their genetic basis is constantly changing and presents differently in individual patients. In the future, SNAs may be used as on-demand individualized therapeutic options for several diseases.

The economic benefit of SNA-based therapy is considerable and rapidly growing. Several companies such as AuraSense Therapeutics and Nanosphere have been founded on the basis of SNA technology, and several types of SNAs have been shown to be well tolerated in clinical Phase I trials. These observations strongly encourage the development of further SNA-based therapeutics.

Outstanding Questions

Do different core materials have differential effects on SNA functions? Do they have different toxic effects on cells?

Which method of synthesis is the best to enhance SNA stability *in vivo*?

Can SNAs be used to achieve efficient gene regulation *in vivo*?

What types of SNA NP formulations are most efficient under *in vivo* conditions?

What is the optimal therapeutic window for the application of SNAs?

Acknowledgments

The authors are grateful for financial support from the Immunology Research Center, Tabriz University of Medical Sciences. Carol Kelly is thanked for assistance in manuscript preparation.

Supplemental Information

Supplemental information associated with this article can be found online at <https://doi.org/10.1016/j.molmed.2019.08.012>.

References

- Cutler, J.I. *et al.* (2012) Spherical nucleic acids. *J. Am. Chem. Soc.* 134, 1376–1391
- Sun, J. *et al.* (2016) Highly hybridizable spherical nucleic acids by tandem glutathione treatment and polythymine spacing. *ACS Appl. Mater. Interfaces* 8, 12504–12513
- Cutler *et al.* (2011) Polyvalent nucleic acid nanostructures. *J. Am. Chem. Soc.* 133, 9254–9257
- Wang, L. *et al.* (2019) Poly-adenine-mediated spherical nucleic acids for strand displacement-based DNA/RNA detection. *Biosens. Bioelectron.* 127, 85–91
- Guan, C. *et al.* (2018) RNA-based immunostimulatory liposomal spherical nucleic acids as potent TLR7/8 modulators. *Small* 14, e1803284
- Zhu, D. *et al.* (2018) Poly-adenine-mediated fluorescent spherical nucleic acid probes for live-cell imaging of endogenous tumor-related mRNA. *Nanomedicine* 14, 1797–1807
- Rouge, J.L. *et al.* (2015) Ribozyme–spherical nucleic acids. *J. Am. Chem. Soc.* 137, 10528–10531
- Massich, M.D. *et al.* (2010) Cellular response of polyvalent oligonucleotide–gold nanoparticle conjugates. *ACS Nano* 4, 5641–5646
- Massich, M.D. *et al.* (2009) Regulating immune response using polyvalent nucleic acid–gold nanoparticle conjugates. *Mol. Pharm.* 6, 1934–1940
- Zheng, D. *et al.* (2012) Topical delivery of siRNA-based spherical nucleic acid nanoparticle conjugates for gene regulation. *Proc. Natl. Acad. Sci. U.S.A.* 109, 11975–11980
- Li, H. *et al.* (2018) Molecular spherical nucleic acids. *Proc. Natl. Acad. Sci. U.S.A.* 115, 4340–4344
- Seferos, D.S. *et al.* (2008) Polyvalent DNA nanoparticle conjugates stabilize nucleic acids. *Nano Lett.* 9, 308–311
- Patel, P.C. *et al.* (2010) Scavenger receptors mediate cellular uptake of polyvalent oligonucleotide-functionalized gold nanoparticles. *Bioconjug. Chem.* 21, 2250–2256
- Choi, C.H.J. *et al.* (2013) Mechanism for the endocytosis of spherical nucleic acid nanoparticle conjugates. *Proc. Natl. Acad. Sci. U.S.A.* 110, 7625–7630
- Mirkin, C.A. *et al.* (1996) A DNA-based method for rationally assembling nanoparticles into macroscopic materials. *Nature* 382, 607
- Zhang, C. *et al.* (2015) Biodegradable DNA-brush block copolymer spherical nucleic acids enable transfection agent-free intracellular gene regulation. *Small* 11, 5360–5368
- Zhu, S. *et al.* (2018) PLGA spherical nucleic acids. *Adv. Mater.* 1707113
- Melamed, J.R. *et al.* (2018) Spherical nucleic acid architecture can improve the efficacy of polycation-mediated siRNA delivery. *Mol. Ther. Nucleic Acids* 12, 207–219
- Liu, B. *et al.* (2018) Polyvalent spherical nucleic acids for universal display of functional DNA with ultrahigh stability. *Angew. Chem. Int. Ed. Engl.* 57, 9439–9442
- Krishnamoorthy, K. *et al.* (2018) Defining the structure of a protein–spherical nucleic acid conjugate and its counterionic cloud. *ACS Cent. Sci.* 4, 378–386
- Letsinger, R. *et al.* (2000) Use of a steroid cyclic disulfide anchor in constructing gold nanoparticle–oligonucleotide conjugates. *Bioconjug. Chem.* 11, 289–291
- Randeria, P.S. *et al.* (2015) Nanoflares as probes for cancer diagnostics. In *Nanotechnology-Based Precision Tools for the Detection and Treatment of Cancer*, C.A. Mirkin *et al.*, eds. (Springer), pp. 1–22
- Hill, H.D. *et al.* (2009) The role radius of curvature plays in thiolated oligonucleotide loading on gold nanoparticles. *ACS Nano* 3, 418–424
- Liu, B. *et al.* (2018) Bromide as a robust backfiller on gold for precise control of DNA conformation and high stability of spherical nucleic acids. *J. Am. Chem. Soc.* 140, 4499–4502
- Ferns, G. (1973) Controlled nucleation for the regulation of particle size in monodisperse gold solutions. *Nature* 241, 20–22
- Gudipati, S. *et al.* (2019) Towards self-transfecting nucleic acid nanostructures for gene regulation. *Trends Biotechnol.* 37, 983–994
- Narayan, S.P. *et al.* (2015) The sequence-specific cellular uptake of spherical nucleic acid nanoparticle conjugates. *Small* 11, 4173–4182
- Peterson, A.W. *et al.* (2001) The effect of surface probe density on DNA hybridization. *Nucleic Acids Res.* 29, 5163–5168
- Hurst, S.J. *et al.* (2006) Maximizing DNA loading on a range of gold nanoparticle sizes. *Anal. Chem.* 78, 8313–8318
- Lytton-Jean, A.K. and Mirkin, C.A. (2005) A thermodynamic investigation into the binding properties of DNA functionalized gold nanoparticle probes and molecular fluorophore probes. *J. Am. Chem. Soc.* 127, 12754–12755
- Yao, D. *et al.* (2015) Integrating DNA-strand-displacement circuitry with self-assembly of spherical nucleic acids. *J. Am. Chem. Soc.* 137, 14107–14113
- Song, W.C. *et al.* (2017) Backbone-modified oligonucleotides for tuning the cellular uptake behaviour of spherical nucleic acids. *Biomater. Sci.* 5, 412–416
- Monopoli, M.P. *et al.* (2011) Physical–chemical aspects of protein corona: relevance to in vitro and in vivo biological impacts of nanoparticles. *J. Am. Chem. Soc.* 133, 2525–2534
- Ke, P.C. *et al.* (2017) A decade of the protein corona. *ACS Nano* 11, 11773–11776
- Hirsh, S.L. *et al.* (2013) The Vroman effect: competitive protein exchange with dynamic multilayer protein aggregates. *Colloids Surf. B Biointerfaces* 103, 395–404
- Rahman, M. *et al.* (2013) Nanoparticle and protein corona. In *Protein–Nanoparticle Interactions*, M. Rahman *et al.*, eds. (Springer), pp. 21–44

37. Nguyen, V.H. and Lee, B.-J. (2017) Protein corona: a new approach for nanomedicine design. *Int. J. Nanomed.* 12, 3137–3151
38. Tenzer, S. et al. (2013) Rapid formation of plasma protein corona critically affects nanoparticle pathophysiology. *Nat. Nanotechnol.* 8, 772–781
39. Zhdanov, V.P. (2019) Formation of a protein corona around nanoparticles. *Cur. Opin. Colloid Interface Sci.* 41, 95–103
40. Mahmoudi, M. et al. (2016) Emerging understanding of the protein corona at the nano–bio interfaces. *Nano Today* 11, 817–832
41. Walkey, C.D. and Chan, W.C. (2012) Understanding and controlling the interaction of nanomaterials with proteins in a physiological environment. *Chem. Soc. Rev.* 41, 2780–2799
42. Koegler, P. et al. (2012) The influence of nanostructured materials on biointerfacial interactions. *Adv. Drug Deliv. Rev.* 64, 1820–1839
43. Mosquera, J.S. et al. (2018) Cellular uptake of gold nanoparticles triggered by host–guest interactions. *J. Am. Chem. Soc.* 140, 4469–4472
44. Lesniak, A. et al. (2013) Nanoparticle adhesion to the cell membrane and its effect on nanoparticle uptake efficiency. *J. Am. Chem. Soc.* 135, 1438–1444
45. Guan, C.M. et al. (2019) Impact of sequence specificity of spherical nucleic acids on macrophage activation in vitro and in vivo. *Mol. Pharm.* 16, 4223–4229
46. Platt, N. and Gordon, S. (2001) Is the class A macrophage scavenger receptor (SR-A) multifunctional? The mouse's tale. *J. Clin. Invest.* 108, 649–654
47. Chinen, A.B. et al. (2015) Spherical nucleic acid nanoparticle conjugates enhance G-quadruplex formation and increase serum protein interactions. *Angew. Chem. Int. Ed. Engl.* 54, 527–531
48. Chinen, A.B. et al. (2017) The impact of protein corona formation on the macrophage cellular uptake and biodistribution of spherical nucleic acids. *Small* 13, 1603847
49. Jokerst, J.V. et al. (2011) Nanoparticle PEGylation for imaging and therapy. *Nanomedicine* 6, 715–728
50. Weissig, V. et al. (2014) Nanopharmaceuticals (part 1): products on the market. *Int. J. Nanomed.* 9, 4357
51. Huckaby, J.T. and Lai, S.K. (2018) PEGylation for enhancing nanoparticle diffusion in mucus. *Adv. Drug Deliv. Rev.* 124, 125–139
52. Zou, W. (2018) Mechanistic insights into cancer immunity and immunotherapy. *Cell. Mol. Immunol.* 15, 419–420
53. Chinen, A.B. et al. (2016) Relationships between poly(ethylene glycol) modifications on RNA–spherical nucleic acid conjugates and cellular uptake and circulation time. *Bioconjug. Chem.* 27, 2715–2721
54. Banga, R.J. et al. (2014) Liposomal spherical nucleic acids. *J. Am. Chem. Soc.* 136, 9866–9869
55. Mokhtarzadeh, A. et al. (2017) Biodegradable nanoparticles as delivery vehicles for therapeutic small non-coding ribonucleic acids. *J. Control. Release* 245, 116–126
56. Yu, Y. and Cui, J. (2018) Present and future of cancer immunotherapy: a tumor microenvironmental perspective. *Oncol. Lett.* 16, 4105–4113
57. Soltani, F. et al. (2015) Synthetic and biological vesicular nano-carriers designed for gene delivery. *Curr Pharm. Design* 21, 6214–6235
58. Bessis, N. et al. (2004) Immune responses to gene therapy vectors: influence on vector function and effector mechanisms. *Gene Therapy* 11, S10
59. Sharon, D. and Kamen, A. (2018) Advancements in the design and scalable production of viral gene transfer vectors. *Biotech. Bioeng.* 115, 25–40
60. Ruan, W. et al. (2018) DNA nanoclew templated spherical nucleic acids for siRNA delivery. *Chem. Commun.* 54, 3609–3612
61. Hargraves, K.G. et al. (2016) Phytochemical regulation of the tumor suppressive microRNA, miR-34a, by p53-dependent and independent responses in human breast cancer cells. *Mol. Carcinogen.* 55, 486–498
62. Rokavec, M. et al. (2014) IL-6R/STAT3/miR-34a feedback loop promotes EMT-mediated colorectal cancer invasion and metastasis. *J. Clin. Invest.* 124, 1853–1867
63. Sita, T.L. et al. (2017) Dual bioluminescence and near-infrared fluorescence monitoring to evaluate spherical nucleic acid nanoconjugate activity in vivo. *Proc. Natl. Acad. Sci. U S A* 114, 4129–4134
64. Slabáková, E. et al. (2017) Alternative mechanisms of miR-34a regulation in cancer. *Cell Death Dis.* 8, e3100
65. Zhao, J. et al. (2017) Synergy between next generation EGFR tyrosine kinase inhibitors and miR-34a in the inhibition of non-small cell lung cancer. *Lung Cancer* 108, 96–102
66. Li, X. et al. (2014) MicroRNA-34a: a potential therapeutic target in human cancer. *Cell Death Dis.* 5, e1327
67. Li, H. et al. (2017) Delivery and release of microRNA-34a into MCF-7 breast cancer cells using spherical nucleic acid nanocarriers. *New J. Chem.* 41, 5255–5258
68. Zheng, J. et al. (2013) A spherical nucleic acid platform based on self-assembled DNA biopolymer for high-performance cancer therapy. *ACS Nano* 7, 6545–6554
69. Wang, X. et al. (2016) Spherical nucleic acid targeting microRNA-99b enhances intestinal MFG-E8 gene expression and restores enterocyte migration in lipopolysaccharide-induced septic mice. *Sci. Rep.* 6, 31687
70. Alhasan, A.H. et al. (2014) Exosome encased spherical nucleic acid gold nanoparticle conjugates as potent microRNA regulation agents. *Small* 10, 186–192
71. Bousmail, D. et al. (2017) Precision spherical nucleic acids for delivery of anticancer drugs. *Chem. Sci.* 8, 6218–6229
72. Tan, X. et al. (2016) Blurring the role of oligonucleotides: spherical nucleic acids as a drug delivery vehicle. *J. Am. Chem. Soc.* 138, 10834–10837
73. Liu, B. and Liu, J. (2017) Freezing directed construction of bio/nano interfaces: reagentless conjugation, denser spherical nucleic acids, and better nanoflares. *J. Am. Chem. Soc.* 139, 9471–9474
74. Banga, R.J. et al. (2017) Drug-loaded polymeric spherical nucleic acids: enhancing colloidal stability and cellular uptake of polymeric nanoparticles through DNA surface-functionalization. *Biomacromolecules* 18, 483–489
75. Prigodich, A.E. et al. (2012) Multiplexed nanoflares: mRNA detection in live cells. *Anal Chem* 84, 2062–2066
76. Yeo, D.C. et al. (2018) Abnormal scar identification with spherical-nucleic-acid technology. *Nat. Biomed. Eng.* 2, 227
77. Lin, M. et al. (2019) Photo-activated nanoflares for mRNA detection in single living cells. *Anal. Chem.* 91, 2021–2027
78. Yan, R. et al. (2018) A nanoflare-based strategy for in situ tumor margin demarcation and neoadjuvant gene/photothermal therapy. *Small* 14, 1802745
79. Alhasan, A.H. et al. (2012) Scanometric microRNA array profiling of prostate cancer markers using

- spherical nucleic acid–gold nanoparticle conjugates. *Anal. Chem.* 84, 4153–4160
80. Alhasan, A.H. et al. (2016) Circulating microRNA signature for the diagnosis of very high-risk prostate cancer. *Proc. Natl. Acad. Sci. U S A* 113, 10655–10660
 81. Halo, T.L. et al. (2014) Nanoflares for the detection, isolation, and culture of live tumor cells from human blood. *Proc. Natl. Acad. Sci. U S A* 111, 17104–17109
 82. Liu, Z. et al. (2018) Cross-platform cancer cell identification using telomerase-specific spherical nucleic acids. *ACS Nano* 12, 3629–3637
 83. Joo, J.H. and Lee, J.S. (2015) Divalent metal ion-mediated assembly of spherical nucleic acids: the case study of Cu^{2+} . *Phys. Chem. Phys.* 17, 30292–30299
 84. Iwasaki, A. and Medzhitov, R. (2004) Toll-like receptor control of the adaptive immune responses. *Nat. Immunol.* 5, 987–995
 85. Banga, R.J. et al. (2017) Cross-linked micellar spherical nucleic acids from thermoresponsive templates. *J. Am. Chem. Soc.* 139, 4278–4281
 86. Radovic-Moreno, A.F. et al. (2015) Immunomodulatory spherical nucleic acids. *Proc. Natl. Acad. Sci. U S A* 112, 3892–3897
 87. Skakuj, K. et al. (2018) Conjugation chemistry-dependent T-cell activation with spherical nucleic acids. *J. Am. Chem. Soc.* 140, 1227–1230
 88. Meckes, B. et al. (2018) Enhancing the stability and immunomodulatory activity of liposomal spherical nucleic acids through lipid-tail DNA modifications. *Small* 14, 1702909
 89. Kouri, F.M. et al. (2015) miRNA-182 and the regulation of the glioblastoma phenotype – toward miRNA-based precision therapeutics. *Cell Cycle* 14, 3794–3800
 90. Kouri, F.M. et al. (2015) MiR-182 integrates apoptosis, growth, and differentiation programs in glioblastoma. *Genes Dev.* 29, 732–745
 91. Sprangers, A.J. et al. (2017) Liposomal spherical nucleic acids for regulating long noncoding RNAs in the nucleus. *Small* 13, 1602753
 92. Randeria, P.S. et al. (2015) siRNA-based spherical nucleic acids reverse impaired wound healing in diabetic mice by ganglioside GM3 synthase knockdown. *Proc. Natl. Acad. Sci. U S A* 112, 5573–5578
 93. Nemati, H. et al. (2017) Using siRNA-based spherical nucleic acid nanoparticle conjugates for gene regulation in psoriasis. *J. Control. Release* 268, 259–268
 94. Barnaby, S.N. et al. (2014) Probing the inherent stability of siRNA immobilized on nanoparticle constructs. *Proc. Natl. Acad. Sci. U S A* 111, 9739–9744
 95. Jensen, S.A. et al. (2013) Spherical nucleic acid nanoparticle conjugates as an RNAi-based therapy for glioblastoma. *Sci. Trans. Med.* 5, 209ra152
 96. Dhar, S. et al. (2010) Polyvalent oligonucleotide gold nanoparticle conjugates as delivery vehicles for platinum (IV) warheads. *J. Am. Chem. Soc.* 132, 2845
 97. Zhang, X.Q. et al. (2011) Strategy for increasing drug solubility and efficacy through covalent attachment to polyvalent DNA–nanoparticle conjugates. *ACS Nano* 5, 6962–6970
 98. Narayan, S.P. et al. (2015) The sequence-specific cellular uptake of spherical nucleic acid nanoparticle conjugates. *Small* 11, 4173–4182
 99. Li, H. et al. (2018) pH-responsive spherical nucleic acid for intracellular lysosome imaging and an effective drug delivery system. *Chem. Commun. (Camb)* 54, 3520–3523